J. Electroanal. Chem., 100 (1979) 583—605

NUMERICAL ANALYSIS OF ELECTRICAL RESPONSE

BIASED SMALL-SIGNAL A.C. RESPONSE FOR SYSTEMS WITH ONE OR TWO BLOCKING ELECTRODES

DONALD R. FRANCESCHETTI and J. ROSS MACDONALD

Department of Physics and Astronomy, University of North Carolina, Chapel Hill, NC 27514 (U.S.A.)

(Received 8th January 1979)

ABSTRACT

The small-signal a.c. response of systems with two blocking electrodes, or one blocking and one ohmic electrode, subject to an external steady voltage bias is examined. The electrolyte is unsupported and may contain one or two mobile charge carrier species. The small-signal response displays features which are readily associated with the redistribution of charge within the system caused by the external bias and the injection of charge into a system with one non-blocking electrode. A procedure is given for approximating the small-signal response of a system containing many Debye lengths from the small-signal response of a thinner system. In addition to describing the impedance and admittance of an initially flat-band system subject to an external bias, the results obtained are also applicable to a limiting case of an unbiased system with intrinsic space charge (Frenkel) layers. An equivalent circuit is found which usually provides an adequate approximate representation of the system response, and the physical interpretation of the circuit parameters is discussed.

(I) INTRODUCTION

Most theoretical treatments of the electrical response of electrode/material/electrode systems (in which the electrodes are metallic and the material is a semiconductor or ionic conductor) are based upon a mathematical model in which the transport of charge through the material is governed by a set of coupled non-linear differential equations, subject to boundary conditions which characterize the material/electrode interface. From the standpoint of solving the equations of the model, the general problem of system response to electrical perturbations may be divided into three separate cases: the steady state, small displacements from a steady state (the small-signal case), and large displacements from steady state conditions (the large-signal case). In systems with at least one completely blocking electrode, the steady-state characteristics can often be expressed in closed analytical form [1—5]. The small-signal problem, for which the equations of the model may be linearized, is amenable to exact analytical treatment under somewhat broader, though still rather restrictive conditions [6,7]. In general, however, analysis of the steady state, small- or large signal cases requires the solution of the relevant equations by approximate numerical methods, and quite a number of papers dealing with numerical techniques may be found in the recent electrochemical [8—11] and semiconductor literature [12—16].

In recent work [7], the present authors obtained exact expressions for the response of an electrode/material/electrode system to small a.c. perturbations, provided that the system is flat-band (i.e. is unbiased and lacks intrinsic space charge layers), contains no more species of mobile charge (as in an unsupported electrolyte), and has bulk generation/recombination and electrode adsorption/ reaction processes which meet well defined but fairly general criteria. Not infrequently, however, measurements of small-signal response are made both at zero and at finite biasing potentials [17—21]. Further, although it can be hoped that in many cases intrinsic space charge layers can be neglected, the probable presence of a static space charge layer at an interface, even one with a blocking electrode, should be taken into account in a comprehensive theoretical treatment. In the present work we have employed numerical techniques to examine the small-signal response of systems subject to a steady d.c. bias. Some of the results obtained are also pertinent to limiting instances of unbiased systems with intrinsic space charge layers. In addition to discussing the method employed and presenting the results obtained, we shall consider below a possible method for fitting experimental data to our numerical results.

For clarity this paper is divided into sections. In Section II the basic equations of the model are summarized in both conventional and normalized form. A brief discussion of the steady state characteristics which enter into the small-signal calculation is given in Section III. In Section IV the equations determining small-signal response are obtained and the method of numerical solution is discussed. In Section V we consider the small-signal response of systems with a single blocking electrode and a reversible ohmic electrode. In addition to characterizing such systems in themselves, the results obtained here allow us to formulate accurate small-signal response results for systems with many (>100) Debye lengths between two blocking electrodes and which either (a) are subject to a d.c. bias or (b) have intrinsic space charge layers in the equilibrium state. The impedance and admittance of thinner systems with two blocking electrodes are examined in Section VI. In Section VII we examine the utility of the results obtained here in the interpretation of experimental data. A final Section provides a summary and indicates possible directions for future work.

(II) GENERAL EQUATIONS

We consider a homogeneous slab of material, a single crystal or homogeneous solution, of length l, extending between two plane-parallel electrodes. We neglect possible edge and magnetic field effects and consider an effectively one-dimensional system. All subsequent analysis will deal with a unit cross-sectional area of this system. The material is assumed to contain a single species of positive mobile charge carrier and a single species of negative mobile charge carrier. The concentrations of these species will be denoted $p(x)$ and $n(x)$, respectively. Symbols not defined here have their conventional meanings and are found in previous work on large-signal transient response [5]. The flux densities of the two charge species are assumed to obey the Nernst-Planck equations:

$$J_p = \mu_p pE - D_p \frac{\partial p}{\partial x} \tag{1}$$

and

$$J_n = -\mu_n n E - D_n \frac{\partial n}{\partial x} \tag{2}$$

It will be assumed throughout this work that the charge mobilities, μ_p and μ_n, and diffusion coefficients, D_p and D_n, are field and concentration independent and that the diffusion coefficients are related to the mobilities through the familiar Einstein relations, $D_p = (\mu_p k_B/z_p e)$ and $D_n = (\mu_n k_B/z_n e)$.

The behavior of the system is further determined by Poisson's equation

$$\frac{\partial E}{\partial x} = \frac{4\pi e}{\epsilon}(z_p p - z_n n + \rho_0) \tag{3}$$

when ρ_0 is the density of immobile background charge, if any is present; by the equations of continuity

$$\frac{\partial p}{\partial t} = -\frac{\partial J_p}{\partial x} \tag{4}$$

and

$$\frac{\partial n}{\partial t} = -\frac{\partial J_n}{\partial x} \tag{5}$$

and by the Maxwell equation

$$I = z_p e J_p - z_n e J_n + \frac{\epsilon}{4\pi}\frac{\partial E}{\partial x} \tag{6}$$

We shall consider the left-hand electrode to be at a potential V_a with respect to the right-hand electrode and thus will require that

$$V_a = \int_{-l/2}^{l/2} E \, dx \tag{7}$$

For maximum generality it is desirable to employ a set of normalized, dimensionless variables. In this work we shall make use of the same normalization as in our previous paper on the numerical simulation of electrical response [5], and we only mention the major features of the normalization here. Positions are normalized with respect to the bulk Debye length,

$$L_D \equiv [\epsilon k_B \theta / 4\pi e^2 (z_n^2 n_e + z_p^2 p_e)]^{1/2} \tag{8}$$

and the total normalized distance between electrodes is denoted as $2M$, where $M \equiv l/2L_D$. For systems in which only one species is mobile a more natural unit of length is

$$L_{D_1} \equiv [\epsilon k_B \theta / 4\pi e^2 z_m^2 c_m]^{1/2} \tag{9}$$

where z_m and c_m are the charge and concentration of the single mobile species. In the present work, however, the normalized half-length of the material will be given as M, rather than $M_1 \equiv l/2L_{D_1}$, to facilitate comparisons with the two-mobile case. The electrostatic potential is normalized with respect to the thermal voltage, $V^* \equiv V/(k_B\theta/e)$. The applied potential, V_a, is considered to lie in the small-signal regime when $|V_a^*| << 1$. For convenience of reference we give the normalized forms of eqns. (1)—(7) below:

$$J_p^* = z_p PE^* - \frac{\partial P}{\partial X} \tag{10}$$

$$J_n^* = -z_n NE^* - \frac{\partial N}{\partial X} \tag{11}$$

$$\frac{\partial E^*}{\partial X} = \delta_p P - \delta_n N - \nu \tag{12}$$

$$\lambda_p \frac{\partial P}{\partial T} = -\frac{\partial J_p^*}{\partial X} \tag{13}$$

$$\lambda_n \frac{\partial N}{\partial T} = -\frac{\partial J_n^*}{\partial X} \tag{14}$$

$$I^* = \epsilon_p J_p^* - \epsilon_n J_n^* + \frac{\partial E^*}{\partial T} \tag{15}$$

$$V_a^* = \int_{-M}^{M} E^* \, dX \tag{16}$$

In discussing small-signal response we shall follow the normalization conventions established in our earlier analytic work [6,7]. We shall thus normalize angular frequency ω with the dielectric relaxation time, $\Omega \equiv \omega\tau_D$, impedance with the limiting high frequency resistance of the system, $Z_N \equiv Z/R_\infty$, and capacitance with the geometric capacitance of the system, $C_N \equiv C/C_g$.

(III) STEADY STATE

We shall here adopt the condensed notation (ρ_L, ρ_R, M, π_m, V_{as}^*) to designate the normalized parameters of a given system subject to a given steady applied potential difference. Here $\rho_L = 0$ if the left-hand electrode blocks the flow of positive and negative mobile carriers and $\rho_L = \infty$ if the left-hand electrode is ohmic to the mobile carriers (i.e. allows infinitely rapid charge transfer and preserves the equilibrium bulk value of the charge carrier concentration). The parameter ρ_R denotes the corresponding property of the right-hand electrode. We shall not in this work treat systems in which an electrode is partially polarizable or is blocking to only one species of charge carrier. As defined above, M is one-half the distance between the electrodes, expressed in units of L_D. The quantity $\pi_m \equiv \mu_n/\mu_p$ denotes the ratio of the charge carrier mobilities. Finally, V_{as}^* is the normalized static potential of the left hand electrode with respect to the right hand electrode.

The blocking-electrode steady state conditions are given by eqns. (10)—(12) and (16), with $J_p^* = J_n^* = 0$. When no current flows, the steady state is one of thermal equilibrium. We have previously given [5] a treatment of the steady state for the case of two blocking electrodes based on the earlier analytic work of Jaffé [1] and Macdonald [2—4]. Only minor modifications of this treatment are required to deal with the case in which one of the electrodes is completely blocking and the other is reversible to one or both of the charge carrier species.

The solution of the steady-state equations requires the evaluation of three integration constants in the general case in which both charge species are mobile; only two constants are required when only one species of charge is mobile. The requirement that the total potential drop across the system has the desired value provides one equation for the evaluation of these constants. A second (and third, if needed) equation is provided by the following consideration: if both electrodes are blocking to a given mobile species then the total amount of that species is conserved. If one of the electrodes is reversible to that species then the electrochemical potential of the species must be constant throughout the system.

It will be convenient to separate our discussion of the general (ρ_L, ρ_R, M, π_m, V^*_{as}) case into a treatment of two-mobile systems, for which $0 < \pi_m < \infty$, and a separate treatment of the one-mobile situation in which $\pi_m = 0$ or $\pi_m = \infty$. We restrict our study of the two-mobile case to systems in which there is no net immobile background charge. The general two-mobile case, with non-zero immobile charge density falls logically between the two-mobile and one-mobile situations considered here.

We first deal with the (0, 0, M, π_m, V^*_{as}) two-mobile situation, for which it is convenient to let the potentials of the left and right electrodes be $V^*_{as}/2$ and $-V^*_{as}/2$, respectively, and to let the system extend form $X = -M$ to $X = M$. Then for $z_p = z_n = 1$ and in the absence of generation or recombination of the charge carriers, the steady state electrostatic potential, electric field, and charge carrier concentrations are given by [5]

$$V^* = \ln \frac{\mathrm{dn}(XC_0^{1/2}, \kappa) - (1-\kappa^2)^{1/2}\mathrm{sn}(XC_0^{1/2}, \kappa)}{\mathrm{dn}(XC_0^{1/2}, \kappa) + (1-\kappa^2)^{1/2}\mathrm{sn}(XC_0^{1/2}, \kappa)} \tag{17}$$

$$E^* = \frac{[4C_0(1-\kappa^2)]^{1/2}}{\mathrm{cn}(XC_0^{1/2}, \kappa)} \tag{18}$$

$$P = C_0 e^{-V^*} \tag{19}$$

and

$$N = C_0 e^{V^*} \tag{20}$$

where sn, cn and dn are Jacobian elliptic functions [22]. The constant C_0 and the modulus κ must be chosen so that the total amount of each charge species is conserved and V^* takes on its proper values at the electrodes. An algorithm for this purpose was given in our previous paper [5].

We next consider the (0, ∞, M, π_m, V^*_{as}) two-mobile case. Here it is more convenient to take the potential of the left-hand electrode as V^*_{as} and that of the right-hand electrode as zero, and to let the system extend from $X = -2M$ to $X = 0$. Then for the same material the steady state distributions are given by

$$V^* = \ln \frac{\mathrm{dn}(X/2, \kappa) - (1-\kappa^2)^{1/2}\mathrm{sn}(X/2, \kappa)}{\mathrm{dn}(X/2, \kappa) + (1-\kappa^2)^{1/2}\mathrm{sn}(X/2, \kappa)} \tag{21}$$

$$E^* = \frac{[4(1-\kappa)^2]^{1/2}}{\mathrm{cn}(X/2, \kappa)} \tag{22}$$

$$P = \mathrm{e}^{-V^*} \tag{23}$$

and

$$N = \mathrm{e}^{V^*} \tag{24}$$

Here the modulus κ is determined by the requirement that $V^* = V^*_{\mathrm{as}}$ at the left electrode.

It should be noted that the expressions given above for V^* and E^* are not valid if the minimum value of the field, $E^*(X = 0)$ in both cases, is greater than $2C_0^{1/2}$ for two blocking electrodes or greater than 2 for one blocking and one reversible electrode. This situation is primarily of interest for systems of very small M and need not concern us further in this work.

The steady state differential capacitance,

$$C_{\mathrm{d}} \equiv \frac{\mathrm{d}q}{\mathrm{d}V_{\mathrm{as}}} \tag{25}$$

is also of interest in regard to biased small-signal response. Here q is the magnitude of the charge on the blocking electrode and V_{as} is the (unnormalized) applied potential difference. C_{d} may be calculated from the dependence of the electric field at a blocking electrode upon V_{as}. In the case of two blocking electrodes, this calculation requires the iterative determination of the constants C_0 and κ in eqn. (18). In the case of one blocking and one ohmic electrode, however, the modulus κ is very nearly unity for $M \lesssim V^*_{\mathrm{as}}$, and after a number of approximations one obtains the result,

$$C_{\mathrm{dN}} \equiv C_{\mathrm{d}}/C_{\mathrm{g}} \cong 2M\,\mathrm{ctnh}(M)\cosh(V^*_{\mathrm{as}}/2) \tag{26}$$

We now consider the $(0, 0, M, \pi_{\mathrm{m}}, V^*_{\mathrm{as}})$ one-mobile case, taking $\pi_{\mathrm{m}} = \infty$ and $V^*_{\mathrm{as}} > 0$ for definiteness. As shown by Macdonald [3] the requirements of charge carrier conservation may be met, in the absence of generation/recombination by letting

$$n = \exp(V^*) \tag{27}$$

and setting the potential of the left electrode as $V^*_{\mathrm{as}} - V^*_{\mathrm{d}}$ and the potential of the right electrode as $-V^*_{\mathrm{d}}$ where

$$V^*_{\mathrm{d}} = V^*_{\mathrm{as}} - \ln\{V^*_{\mathrm{as}}/[1 - \exp(-V^*_{\mathrm{as}})]\} \tag{28}$$

The electric field is then given as a function of V^*_{as} by

$$E^* = [c_0 + \exp(V^*) - 1 - V^*]^{1/2} \tag{29}$$

where c_0 is a constant chosen so that

$$2M = \int_{-V^*_{\mathrm{d}}}^{V^*_{\mathrm{as}} - V^*_{\mathrm{d}}} [\mathrm{d}V/E^*(V^*)] \tag{30}$$

Once c_0 is determined, one may readily evaluate n, E^*, and

$$X = \int_{V^*}^{V^*_{as}-V^*_d} [dV^*/E^*(V^*)] - M \tag{31}$$

for any value of V^* between $-V^*_d$ and $V^*_{as} - V^*_d$.

It is a simple matter to modify this procedure to deal with the $(0, \infty, M, \infty, V^*_{as})$ and $(\infty, 0, M, \infty, V^*_{as})$ cases. We first note that for $V^*_{as} > 0$, since only negative charges are mobile, the $(0, \infty, M, \infty, V^*_{as})$ system will exhibit a depletion of the mobile charges near the blocking electrode while the $(\infty, 0, M, \infty, V^*_{as})$ system will show an accumulation of mobile charge at its blocking electrode. For $V^*_{as} <$ 0 the space charge regions will have the opposite character. We will consider explicitly only the $V^*_{as} > 0$ cases. For the $(0, \infty, M, \infty, V^*_{as})$ situation we place the ohmic electrode at $X = 0$ and the blocking electrode at $X = -2M$ while for the $(\infty, 0, M, \infty, V^*_{as})$ system we place the ohmic electrode at $X = 0$ and the blocking electrode at $X = 2M$. The electrostatic field is given by eqn. (25) in both cases and C_0 is determined by

$$2M = \int_0^{V^*_{as}} [dV^*/E^*(V^*)] \tag{32}$$

for the $(0, \infty, M, \infty, V^*_{as})$ situation and by

$$2M = \int_{-V^*_{as}}^{0} [dV^*/E^*(V^*)] \tag{33}$$

in the $(\infty, 0, M, \infty, V^*_{as})$ case. Further

$$X = \int_0^{V^*} [dV^*/E^*(V^*)] \tag{34}$$

in the former instance and

$$X = \int_{V^*-V^*_{as}}^{0} [dV^*/E^*(V^*)] \tag{35}$$

in the latter.

In the one-mobile cases considered here and for $M >> 1$ and $M \gtrsim V^*_{as}$, the quantity c_0 appearing in eqn. (25) is much smaller than the absolute value of V^*_{as}. Under these conditions one may neglect c_0 in evaluating the electric field, and thus the charge, at the electrode, and it is then possible to obtain an analytic approximation for the differential capacitance. In the two blocking-electrode $(0, 0, M, \infty, V^*_{as})$ case the appropriate expression is

$$C_{dN} = \frac{[V^*_{as} - 1 + \exp(-V^*_{as})][1 - (1 + V^*_{as})\exp(-V^*_{as})]M}{V^*_{as}[1 - \exp(-V^*_{as})]\left\{\dfrac{V^*_{as}}{1 - \exp(-V^*_{as})} - 1 - \ln \dfrac{V^*_{as}}{1 - \exp(-V^*_{as})}\right\}^{1/2}} \tag{36}$$

Far simpler results are obtained when one of the electrodes is ohmic. One has

$$C_{\mathrm{dN}} = \frac{|\exp(-V_{\mathrm{as}}^*) - 1|M}{[\exp(-V_{\mathrm{as}}^*) - 1 - V_{\mathrm{as}}^*]^{1/2}} \tag{37}$$

in the $(0, \infty, M, \infty, V_{\mathrm{as}}^*)$ and

$$C_{\mathrm{dN}} = \frac{|\exp(V_{\mathrm{as}}^*) - 1|M}{[\exp(V_{\mathrm{as}}^*) - 1 + V_{\mathrm{as}}^*]^{1/2}} \tag{38}$$

in the $(\infty, 0, M, \infty, V_{\mathrm{as}}^*)$ situation.

In closing our discussion of the steady state it should be noted that the steady state results obtained for systems with an ohmic electrode apply as well if the ohmic electrode is replaced by a reversible electrode ($\rho_{\mathrm{L}}, \rho_{\mathrm{R}} < \infty$), provided that the electrode maintains the bulk equilibrium value of the charge carrier concentrations. The small-signal response of such a system will, however, depend on the rate constants for the electrode reaction.

(IV) SMALL-SIGNAL EQUATIONS

We now assume that the potential difference V_{a}^* applied to the system consists of a steady state part and a small sinusoidal perturbation,

$$V_{\mathrm{a}}^* \equiv V_{\mathrm{as}}^* + V_{\mathrm{a1}}^* \mathrm{e}^{\mathrm{i}\Omega T} \tag{39}$$

Similarly, we decompose each of the independent variables appearing in eqns. (8)—(14) into steady state and sinusoidal components: $P = P_{\mathrm{s}} + P_1 \mathrm{e}^{\mathrm{i}\Omega T}, E^* = E_{\mathrm{s}}^* + E_1^* \mathrm{e}^{\mathrm{i}\Omega T}$, and so on, where the steady state components are given for the appropriate V_{as}^* by the methods of Section III. On inserting these forms into eqns. (8)—(14), dropping terms quadratic in the sinusoidal components and using the steady state conditions to eliminate terms involving the steady state components only, we obtain a set of equations for $P_1, N_1, E_1^*, J_{\mathrm{p1}}^*, J_{\mathrm{n1}}^*, I_1^*$ and V_{a1}^* which are [6]

$$J_{\mathrm{p1}}^* = \left[z_{\mathrm{p}} P_{\mathrm{s}} E_1^* + z_{\mathrm{p}} P_1 E_{\mathrm{s}}^* - \frac{\partial P_1}{\partial X} \right] \tag{40}$$

$$J_{\mathrm{n1}}^* = \left[-z_{\mathrm{n}} N_{\mathrm{s}} E_1^* - z_{\mathrm{n}} N_1 E_{\mathrm{s}}^* - \frac{\partial N_1}{\partial X} \right] \tag{41}$$

$$\frac{\partial E_1^*}{\partial X} = \delta_{\mathrm{p}} P_1 - \delta_{\mathrm{n}} N_1 \tag{42}$$

$$\mathrm{i}\Omega\lambda_{\mathrm{p}} P_1 = -\frac{\partial J_{\mathrm{p1}}^*}{\partial X} \tag{43}$$

$$\mathrm{i}\Omega\lambda_{\mathrm{n}} N_1 = -\frac{\partial J_{\mathrm{n1}}^*}{\partial X} \tag{44}$$

$$I_1^* = \epsilon_{\mathrm{p}} J_{\mathrm{p1}}^* - \epsilon_{\mathrm{n}} J_{\mathrm{n1}}^* + \mathrm{i}\Omega E_1^* \tag{45}$$

and

$$V_{a1}^* = \int_{-M}^{M} E_1^* \, dX \tag{46}$$

Of primary importance in small-signal response is the system impedance, in normalized form $Z_N \equiv V_{a1}^*/(2MI_1^*)$, and its admittance $Y_N \equiv Z_N^{-1}$. These are most easily evaluated by assuming a fixed value for I_1^*, which is spatially invariant in one dimension [23], solving eqns. (40)—(45) for E_1^*, and then evaluating V_{a1}^* from eqn. (46). Since the differential equations for the perturbation components are linear, and our primary goal is to evaluate Z_N and Y_N, one may choose any value for I_1^*. We set $I_1^* = 1$. Analytic solution of eqns. (40)—(45) is possible only in the "flat-band" case, in which P_s, N_s and E_s have constant values. In seeking a numerical solution it is highly desirable to first eliminate as many independent variables as possible from the equations. On combining eqns. (43) and (44) with (40) and (41) and eliminating J_{p1}^*, J_{n1}^* and P_1, one obtains the following two coupled equations.

$$\epsilon_p \frac{d^2E_1^*}{dX^2} = (\epsilon_p z_p \delta_p P_s + \epsilon_n z_n \delta_p N_s)E_1^* + \epsilon_p z_p E_s \frac{dE_1^*}{dX} + (\epsilon_p z_p \delta_n + \epsilon_n z_n \delta_p)E_s^* N_1 + (\epsilon_n \delta_p - \epsilon_p \delta_n) \frac{dN_1}{dX} + i\Omega E_1^* - 1 \tag{47}$$

and

$$i\Omega\lambda_n N_1 = \frac{d}{dX}\left[z_n N_s E_1^* + z_n N_1 E_s^* + \frac{dN_1}{dX}\right] \tag{48}$$

Solution of these equations requires a total of four boundary conditions. The most natural formulation of boundary conditions for a completely blocking electrode is that $J_n^* = J_p^* = 0$ at the electrode surface. For use with eqns. (47) and (48) one has, from eqns. (41) and (45),

$$z_n N_s E_1^* + z_n N_1 E_s^* + \frac{dN_1}{dX} = 0 \tag{49}$$

and

$$i\Omega E_1^* = I_1 \equiv 1 \tag{50}$$

at a blocking electrode. The most natural boundary conditions for an ohmic electrode are obtained from the requirement that the charge carrier concentrations have their bulk equilibrium values at such as electrode. In normalized units one must have $P = 1/z_p$ and $N = 1/z_n$, which in turn require that $dE_1^*/dX = 0$ at the electrode. The latter two conditions on N and E_1 are suitable for use with eqns. (47) and (48).

It is advisable to treat the one-mobile case separately. With $\pi_m = \infty$, for example, one obtains the single equation

$$\epsilon_n \frac{d^2E_1^*}{dX^2} = \epsilon_n z_n \delta_n N_s E_1^* - \epsilon_n z_n E_s^* \frac{dE_1^*}{dX} + i\Omega\delta_n E_1^* - \delta_n \tag{51}$$

which may be solved subject to the boundary conditions $i\Omega E_1^* = 1$ at a blocking electrode and $dE_1^*/dX = 0$ at an ohmic electrode.

For numerical treatment, eqns. (47) and (48) or (51) and the corresponding boundary conditions were separated into real and imaginary parts and the resulting equations solved with the aid of POST, a package of FORTRAN subroutines for the numerical solution of partial and ordinary differential equations, written by Schryer [24]. POST solves ordinary differential equations in one spatial dimension using Galerkin's method with a basis set of B-spline functions [25]. The latter are defined with respect to a set of spatial mesh points provided by the user and are polynomials between the mesh points. We have discussed the selection of B-spline order and spatial mesh in our previous paper [5] and have followed the same general procedure in this work, using splines of order four and a symmetrical spatial mesh of $2N_\Delta + 1$ points with the n-th and $(N_\Delta - 1)$-th interval of the mesh given by

$$\Delta X_n = \frac{M[\exp(n\Lambda - \Lambda)][\exp(\Lambda - 1)]}{2\left[\exp\left(\frac{N_\Delta - 1}{2}\,\Lambda\right) - 1\right]} \qquad (52)$$

For $M = 10$ we set $\Lambda = 0.25$ and found satisfactory results with $12 \leqslant N_\Delta \leqslant 17$. Once the POST program finds a B-spline representation of $E_1^*(X)$, it is integrated to yield V_{a1}^* and thus Z_N, using programs found in the POST subroutine library [26].

(V) ONE BLOCKING ELECTRODE

Before examining specific small-signal results in detail, we should take note of a number of general and rigorous conclusions that follow from the form of the fundamental equations (1)—(7). It follows from the behavior of these equations (with $z_n = z_p$ and $\rho_0 = 0$) under the interchange of charge carrier species, left-hand and right-hand boundary conditions, and reversal of the biasing potential that the small-signal response obtained in the general $(\rho_L, \rho_R, M, \pi_m, V_{as}^*)$ case also applies in the $(\rho_R, \rho_L, M, \pi_m, -V_{as}^*)$, $(\rho_R, \rho_L, M, \pi_m^{-1}, -V_{as}^*)$, and $(\rho_L, \rho_R, M, \pi_m^{-1}, -V_{as}^*)$ situations. A less obvious conclusion, obtained in earlier work [27], is that the normalized impedance Z_N and admittance Y_N of a $(0, \infty, M, \pi_m, 0)$ system are the same as the corresponding quantities for a $(0, 0, 2M, \pi_m, 0)$ system, which are known in exact analytic form.

Although we have been speaking in terms of an externally applied steady state potential difference, the results presented here will also be relevant to systems in which a space charge (Frenkel [28]) layer is formed at the blocking electrode in the absence of an applied steady biasing potential difference. Frenkel layers will be present if there is a difference in the chemical potential of the mobile charge species between the electrode/material interface and the bulk of the material, even if the flow of charge from the interface into the electrode is completely blocked [29]. In the absence of external bias the net charge distributed through the material will be balanced by an opposite charge on the material surface. If one neglects the potential drop across the surface layer and assumes that the interchange of mobile charges between the surface layer and the remainder of the material is extremely slow, then the response obtained for the $(0, \infty, M, \pi_m, V_{as}^*)$ case of an initially flat-band ($V_{as}^* = 0$) system applies as well when there is a Frenkel layer with diffusion potential V_d^* and the applied static potential difference is $V_{as}^* - V_d^*$. In subsequent papers, the present rather stringent idealization of the surface layer will be relaxed, and the more general case will be treated.

Small-signal response calculations were performed for the $(0, \infty, 10, \pi_m, V_{as}^*)$ situation, i.e. systems of normalized half-length 10 with one ohmic electrode and one blocking electrode. With the exception of membrane systems, this is perhaps approaching the lower limit of M for systems of experimental interest; for pure crystalline KCl, in which the charge carriers are Schottky defects, an $M = 10$ system at 800 K would be about 0.6 mm thick. The impedance and admittance results obtained for $M = 10$, however, display the qualitative features to be expected in systems of $M \lesssim 100$ and, as will be shown below, can be used to construct accurate approximations to the impedance and admittance of larger systems.

Calculations were performed for three values of the mobility ratio, $\pi_m = 1, 5, \infty$, and for several values of the applied steady bias, $V_{as}^* = 0, \pm 2.5, \pm 5.0, \pm 7.5$. The results are shown as Nyquist or Cole-Cole type plots in the impedance and admittance planes in Figs. 1—3. The impedance plane plot for $\pi_m = 1$ is given in Fig. 1a. As noted earlier, the curve for the $V_{as}^* = 0$, unbiased, case is precisely the result for the (0, 0, 20, 1, 0) case, for which the exact expression is known. Since the mobility ratio is unity, the small-signal response depends on the absolute value of the bias potential and not on its sign. As $|V_{as}^*|$ increases, the semicircular portion of the curve becomes more complete, an effect which can be attributed to the net injection of charge into the system through the ohmic electrode, reducing the local Debye length. Also, as $|V_{as}^*|$ increases, the vertical portion of the plot (which represents the low frequency response) develops a bend prior to approaching its vertical asymptote at R_{N0}. This non-vertical, roughly linear portion of the curve might be attributed to a diffusion-like effect associated with a net excess of one charge carrier species over the other, an interpretation supported by the absence of a similar feature in the one-mobile case (see below). In the corresponding admittance plane plot (Fig. 1b) the low-frequency behavior

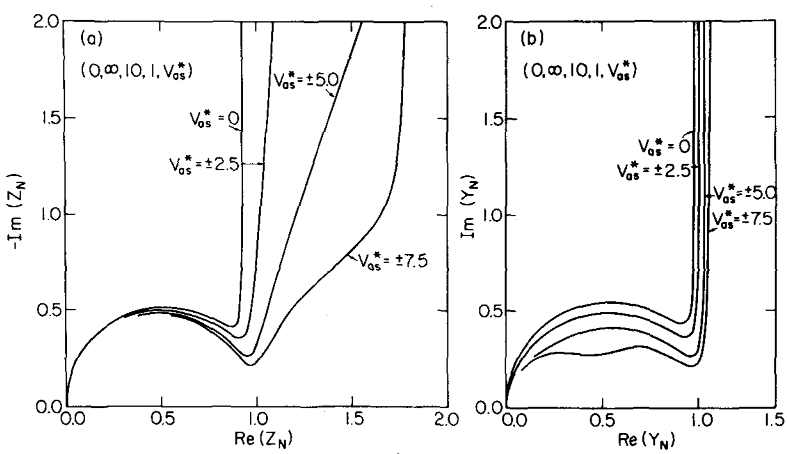

Fig. 1. Impedance (a) and admittance (b) plane plots for $(0, \infty, 10, 1, V_{as}^*)$ systems.

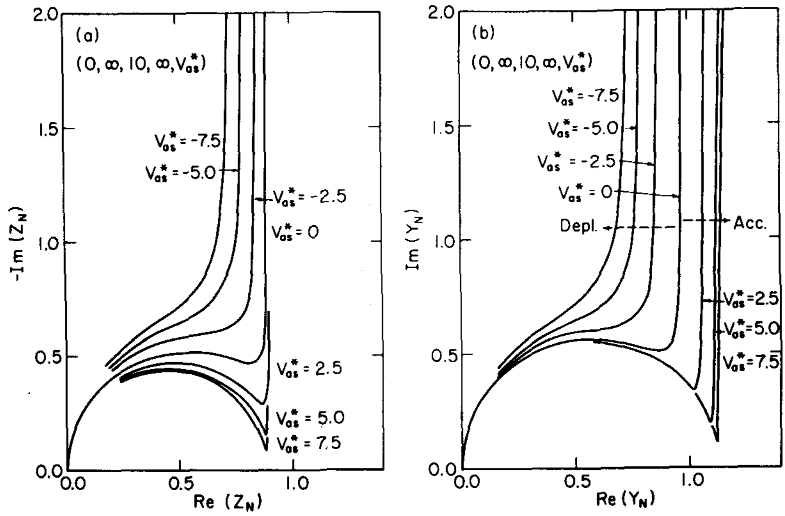

Fig. 2. Impedance (a) and admittance (b) plane plots for (0, ∞, 10, ∞, V_{as}^*) systems.

is represented by the semicircular portion, which becomes deformed as $|V_{as}^*|$ increases. At high frequencies, the response is essentially capacitative, as shown by the nearly straight-line vertical portions of the curves. The vertical asymptotes occur at $G_{N\infty}$, the limiting high frequency conductance, which is unity at $V_{as}^* = 0$ as required by the normalization chosen and increases with $|V_{as}^*|$, reflecting the net injection of mobile charge into the system.

The impedance plane plot for $\pi_m = \infty$ is given in Fig. 2a. In contrast to the $\pi_m = 1$ case, here the system response depends on the sign of V_{as}^* as well as its magnitude. As V_{as}^* increases from $V_{as}^* = 0$, the semicircular portion of the plot is seen to become more complete, reflecting the injection of the mobile negative charge, which accumulates at the blocking electrode. As V_{as}^* decreases below zero the semicircular portion of the plot is diminished, reflecting the extraction

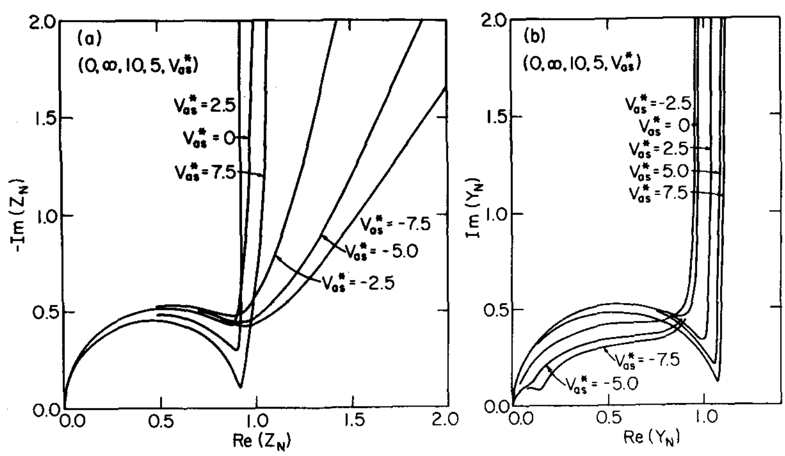

Fig. 3. Impedance (a) and admittance (b) plane plots for (0, ∞, 10, 5, V_{as}^*) systems.

of charge carriers from the system and the formation of a depletion layer at the blocking electrode. Accumulation and depletion effects dominate the admittance plot (Fig. 2b) as well. In particular it should be noted that the vertical asymptote, $G_{N\infty}$, increases as V_{as}^* and the total amount of charge in the system increase.

The impedance plane plot for $\pi_m = 5$ is given in Fig. 3a. The situation here is somewhat more complicated than in the equal-mobility or one-mobile cases, resulting in part from the combination of diffusion-like effects [27,30,31] associated with charge species of different mobilities (even in the unbiased flat-band case) and the consequences of charge injection into the system. All of the curves eventually approach vertical asymptotes as $\Omega \to 0$ at $\mathrm{Re}(Z_N) \equiv R_{N0}$. The complexity of the present case is reflected in the behavior of R_{N0} which is not a monotonic function of V_{as}^* but reaches a minimum near $V_{as}^* = 2.5$. One feature of the plot which is readily understood, however, is the extent of the semicircular component, which markedly approaches a complete semicircle for positive values of V_{as}^*, corresponding to the injection of the more mobile carrier into the system. The admittance plane plot for $\pi_m = 5$ is given in Fig. 3b. We immediately note that the semicircular region becomes more complete as V_{as}^* increases from zero, while as V_{as}^* decreases from zero this region develops additional structure at low frequencies. The vertical asymptote $G_{N\infty}$ takes on its minimum value near $V_{as}^* = -2.5$. The slow increase of $G_{N\infty}$ as V_{as}^* is decreased below this value apparently occurs because the net increase in concentration of the less mobile carrier as V_{as}^* decreases eventually outweighs the depletion of the more mobile carrier, resulting in an increase in the overall conductance of the system.

Although the impedance and admittance plane plots provide a convenient and often highly instructive summary of the system response, the complete specification of the response requires that the components of Z_N or Y_N be determined as functions of frequency. We focus here on the admittance and set

$$Y_N \equiv G_{pN} + i\Omega C_{pN} \tag{53}$$

in the conventional manner. We note first that the limiting values of G_{pN} are zero as $\Omega \to 0$ and $G_{pN\infty}$ as $\Omega \to \infty$, while the corresponding limits of C_{pN} are $C_{dN} \equiv C_{pN0}$ and $C_{gN} \equiv C_{pN\infty} \equiv 1$, respectively.

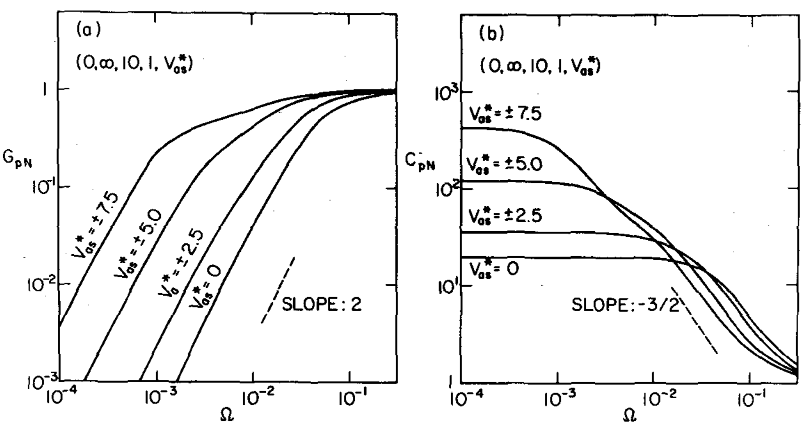

Fig. 4. Frequency dependence of admittance components (eqn. 53) for (0, ∞, 10, 1, V_{as}^*) systems.

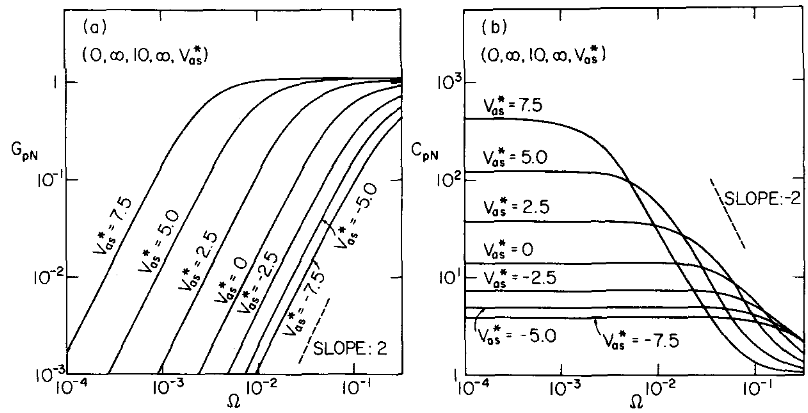

Fig. 5. Frequency dependence of admittance components (eqn. 53) for (0, ∞, 10, ∞, V_{as}^*) systems.

The quantities G_{pN} and C_{pN} are shown in Fig. 4 for the $\pi_m = 1$ case. As noted earlier, the system response depends only on the absolute value of V_{as}^* when the charge carrier mobilities are equal. The $G_{pN}(\Omega)$ and $C_{pN}(\Omega)$ curves have the same general form for $V_{as}^* \neq 0$ as they do in the flat-band case, with some additional structure becoming apparent at high values of $|V_{as}^*|$. Similar qualitative behavior is observed in Fig. 5 for the $\pi_m = \infty$, one-mobile case, with very little change in the form of the curves as V_{as}^* is varied. Here, however, the results for accumulation and depletion situations are indeed well separated, as is expected in the one-mobile case.

In Fig. 6 the quantities G_{pN} and C_{pN} are shown for the $\pi_m = 5$ case. Since in two-mobile systems the differential capacitance C_{dN} is independent of the mobility ratio we find that the C_{pN} curves for V_{as}^* and $-V_{as}^*$ converge as $\Omega \to 0$. As Ω increases the mobility ratio becomes an important factor in determining the system response, with the high-frequency behavior of G_{pN} and C_{pN} acquiring some of the character of the one-mobile case.

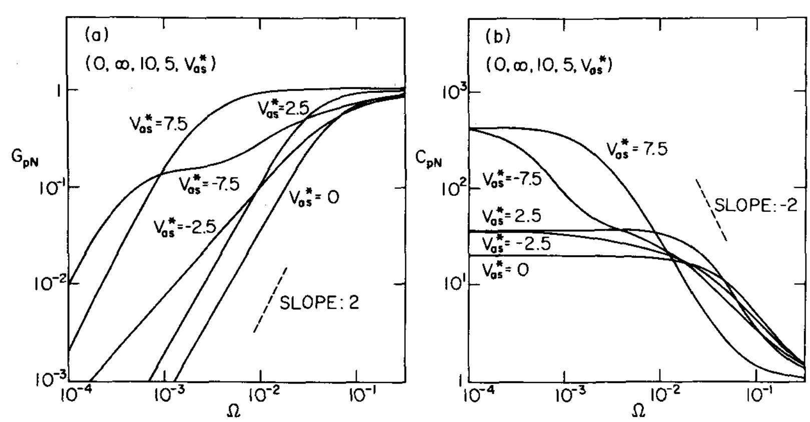

Fig. 6. Frequency dependence of admittance components (eqn. 53) for (0, ∞, 10, 5, V_{as}^*) systems.

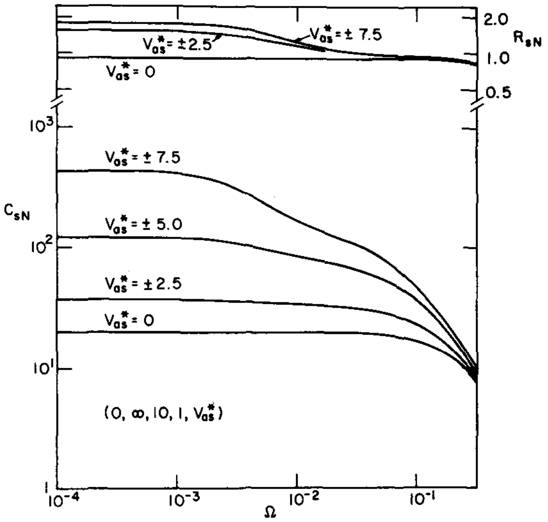

Fig. 7. Frequency dependence of impedance components (eqn. 54) for $(0, \infty, 10, 1, V_{as}^*)$ systems.

It is sometimes also of interest to examine the components of the system impedance

$$Z_N \equiv R_{sN} - i(\Omega C_{sN})^{-1} \tag{54}$$

as functions of frequency. Plots of R_{sN} and C_{sN} as functions of Ω are given in Fig. 7 for the $\pi_m = 1$ case. These curves, and the results for other values of π_m, not shown, reveal that R_{sN} is far less dependent upon frequency or on V_{as}^* than is G_{pN}, while C_{sN} displays a slightly more complex dependence on frequency than does C_{pN}.

The small-signal response results which have been obtained for $M = 10$ systems with one ohmic electrode may, within certain limitations, be combined with other information to provide highly accurate approximations to the small-signal response of larger systems. We expect, for instance, that the impedance of a $(0, \infty, M, \pi_m, V_{as}^*)$ system with $M > 10$ will be well approximated by the sum of the impedance of an $(0, \infty, 10, \pi_m, V_{as}^*)$ system and the impedance of an $(\infty, \infty, M - 10, \pi_m, V_{as}^*)$ system (which is known from the exact small-signal treatment of the flat-band case) as long as $V_{as}^* \lesssim 10$, so that the space charge region which forms at the blocking electrode is almost entirely localized within the 20 Debye lengths nearest the blocking electrode. Similarly one might approximate the response of a $(0, 0, M, \pi_m, V_{as}^*)$ two-mobile system by a series combination of a $(0, \infty, 10, \pi_m, V_{as}^*/2)$ system, a $(\infty, \infty, M - 20, \pi_m, 0)$ system and a $(\infty, 0, 10, \pi_m, V_{as}^*/2)$ system (the latter equivalent to a $(0, \infty, 10, \pi_m, -V_{as}^*/2)$ system). Here it is required that M be sufficiently large ($M \gtrsim 10\ V_{as}^*$) that the depletion of charge from the central region of the material can be neglected and, as before, that V_{as}^* be sufficiently small ($V_{as}^* < 20$). A one-mobile system satisfying the above conditions may be treated as in the two-mobile case, provided that account is taken of the unsymmetrical distribution of the steady state potential drop, as in the discussion of eqn. (24).

As an illustration of this approximate approach, we examine the response of a (0, 0, 1000, 1, V_{as}^*) system. If we let $Z_N(\rho_L, \rho_R, M, \pi_m, V_{as}^*)$ denote the normalized impedance of a system with the indicated parameters we may write

$$Z_N(0, 0, 1000, 1, V_{as}^*) = 0.01Z_N(0, \infty, 10, 1, V_{as}^*/2) + 0.98Z_N(\infty, \infty, 980, 1, 0)$$
$$+ 0.01Z_N(0, \infty, 10, 1, -V_{as}^*/2) \quad (55)$$

with the numerical factors required by the normalization which has been adopted. The central, or bulk, term has a particularly simple form, since

$$Z_N(\infty, \infty, M, \pi_m, 0) = (1 + i\Omega)^{-1} \quad (56)$$

The real part of the bulk contribution will in general dominate the real part of the resultant Z_N. The imaginary part of Z_N will, however, be dominated by the two outer, or interface terms for $\Omega \lesssim 1$. The impedance and admittance plane plots for this $M = 1000$ case show only a slight dependence on V_{as}^*. Nevertheless, when the separate components of Z_N or Y_N are examined, considerable variation with V_{as}^* is found, as is seen in Fig. 8 for G_{pN} and C_{pN}.

(VI) TWO BLOCKING ELECTRODES

We deal in this Section with the (0, 0, M, π_m, V_{as}^*) case, and in particular with systems in which M is too small for the approximate analysis of the preceding Section to be applicable. Small-signal response calculations were performed for the (0, 0, 10, π_m, V_{as}^*) situation with π_m = 1, 5, ∞, as in the previous Section, and for V_{as}^* = 0, ±5, ±10, ±15, and ±20. Since both electrodes are completely blocking in the present case, the system response depends only on the absolute value of V_{as}^*. Impedance and admittance plane plots are given in Figs. 9—11. Although the curves shown in these Figures resemble those of the previous Section in having a semicircular portion and in approaching a vertical asymptote,

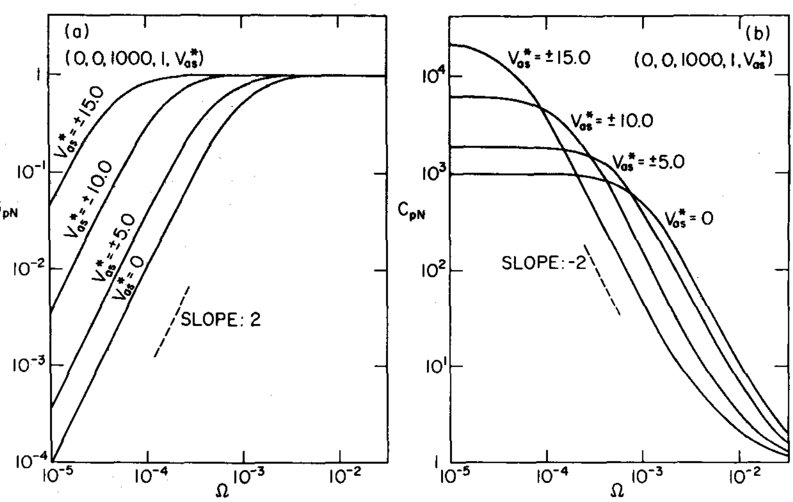

Fig. 8. Frequency dependence of admittance components (eqn. 53) for (0, 0, 1000, 1, V_{as}^*) systems, obtained from eqn. (55).

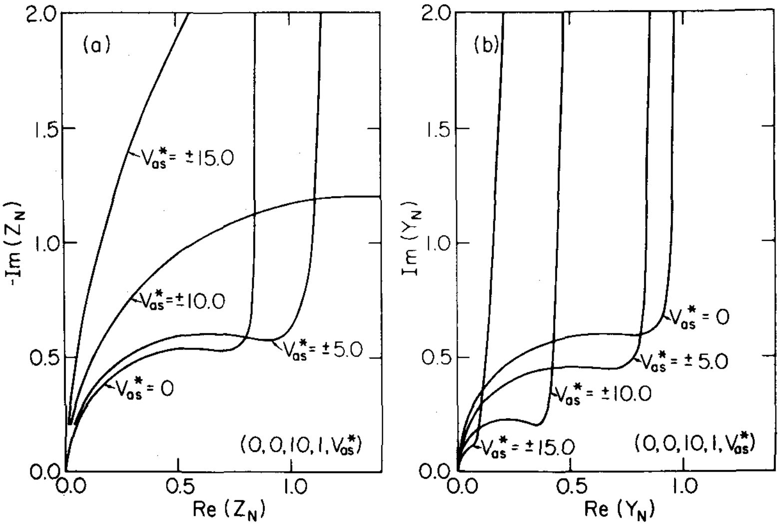

Fig. 9. Impedance (a) and admittance (b) plane plots for (0, 0, 10, 1, V_{as}^{*}) systems.

the curves presented for the two-mobile systems in Figs. 9 and 11 differ in two qualitatively important respects from the corresponding cases in the previous Section. In contrast to the curves obtained for two-mobile systems with one ohmic electrode, the radius of the semicircular portion of the present curves is strongly influenced by V_{as}^{*}. This behavior reflects a significant depletion of charge carrier density from the central portion of the system in the steady state which causes the overall resistance of the system to increase with $|V_{as}^{*}|$ and the conductance to decrease correspondingly. It then follows that the semicircular part of the impedance curves will increase in radius while the semicircular portion of the admittance curves decreases in radius for two-mobile systems. For

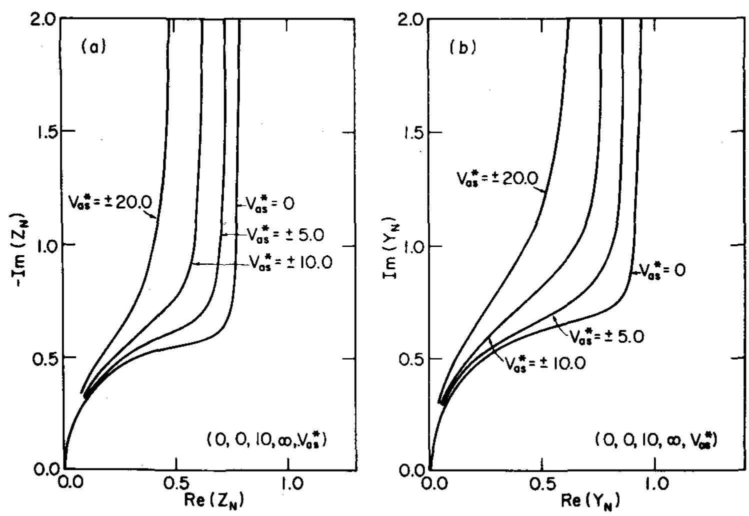

Fig. 10. Impedance (a) and admittance (b) plane plots for (0, 0, 10, ∞, V_{as}^{*}) systems.

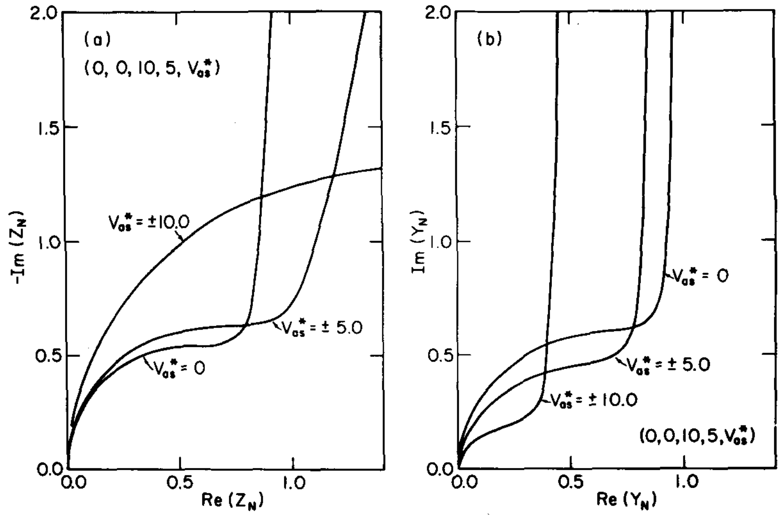

Fig. 11. Impedance (a) and admittance (b) plane plots for (0, 0, 10, 5, V_{as}^*) systems.

the one-mobile system studied there is negligible depletion of charge carrier density in the center of the system and the impedance and admittance curves (Fig. 10) are dominated by the depletion layer which forms at one electrode (compare Fig. 2). The absence of additional features in the vertical portions of the impedance curves of the two-mobile system is the second important difference between the present results and those of the previous Section and is consistent with the interpretation of these features as resulting from the injection of charge into the system, which is, of course, forbidden when both electrodes are blocking.

Rather than presenting graphs of G_{pN} and C_{pN}, or R_{sN} and C_{sN} for the systems studies in this Section we note that since the impedance and admittance results for $V_{as}^* \neq 0$ are qualitatively quite similar to those obtained in the exactly soluble $V_{as}^* = 0$ case, it should be possible to summarize the present results quite concisely through the use of one of the forms of equivalent circuit found applicable in the $V_{as}^* = 0$ case. This possibility is examined in the following section.

(VII) EQUIVALENT CIRCUITS AND DATA ANALYSIS

The primary requirements for an equivalent circuit to fit the data obtained in the preceding two Sections are that it include no path open to current flow at $\Omega = 0$; that it contain a resistive element to allow faradaic current within the material at non-zero frequency; and that it include some Warburg-like element to allow for the effects of arbitrary mobility ratio. The simplest circuit meeting these requirements is that given in Fig. 12, which is a simplified form of a circuit used in earlier work [27]. This circuit includes a finite-length Warburg impedance of the form

$$Z_{DN} = Z_{D0}[\tanh(i\Omega H^2)^{1/2}/(i\Omega H^2)^{1/2}] \qquad (57)$$

as well as the geometric capacitance C_1, bulk resistance R_1 and diffuse layer capacitance C_2. The Warburg impedance (57) is equivalent to a distributed transmission line of length H (in normalized units) terminated by a short [30,31,33].

An attempt was made to determine the best values of the four parameters R_1, C_2, Z_{DO}, and H which best described the impedance and admittance results for each of the systems and bias conditions studied, using a non-linear least squares procedure for the fitting of complex data [32]. In the present work the data were taken at evenly spaced values in log Ω and were weighted equally. The quantity C_1 was held equal to unity in the fit to be reported here; permitting C_1 to vary along with the other parameters produced little improvement in the fit. Representative fitting results for system impedance, Z_N, are given in Table 2, including the estimated uncertainties in the parameters and the estimated standard deviation of the overall fit. Since the equivalent circuit provides only an approximation to the exact result and may deviate from it more in one frequency range than another, the estimated uncertainties and standard deviation have heuristic value but not necessarily rigorous statistical significance.

The fitting results show that the equivalent circuit of Fig. 12 provides a reasonable approximation to the data and that the behavior of the fitting parameters is much as might be expected from the discussions of the previous Sections. The value of C_2 obtained from the fit agrees within 1% with $C_{dN} - 1$, where C_{dN} is the differential capacitance determined by the methods of Section III. The parameter R_1 is found to always increase with $|V_{as}^*|$ in the (0, 0, M, π_m, V_{as}^*) situations, reflecting the combined effects of charge injection and the mobility ratio.

For systems with two blocking electrodes and $\pi_m = 0$ or $\pi_m = \infty$, satisfactory fits are obtained with the finite-length Warburg impedance omitted ($Z_{DO} = 0$), but for $\pi_m = 5$ this component is required. For the (0, 0, 10, 5, V_{as}^*) situation the coefficient Z_{DO} increases with $|V_{as}^*|$ while the effective length H associated with the diffusion effect decreases at high values of $|V_{as}^*|$, probably reflecting the localization of diffusion effects in the space charge layers near the electrode. Previous examination [27] of small-signal results for unbiased systems with two identical electrodes has shown that H is often well approximated by $[0.25(2 + \pi_m + \pi_m^{-1})]^{1/2}M$ for intrinsic materials, in agreement with the value obtained for the (0, 0, 10, 5, 0) case. For (0, ∞, 10, π_m, V_{as}^*) system, with the exception of $\pi_m = \infty$ or ($\pi_m = 0$) and $\pi_m = 1$, $V_{as}^* = 0$, the Warburg impedance is almost always significant, but with the characteristic length H remaining nearly constant at

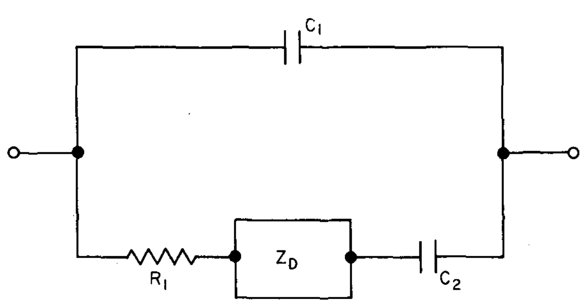

Fig. 12. Approximate equivalent circuit for small-signal response of (0, 0, M, π_m, V_{as}^*) and (0, ∞, M, π_m, V_{as}^*) systems.

TABLE 1

Impedance fitting results for the circuit of Fig. 12

Quantities in parentheses indicate estimated relative standard error of parameters, omitted if less than one part in 10^6

System	R_1	C_2	Z_{D0}	H	s_f
(0, 0, 10, 1, 0)	1.04907 × (1 ± 0.0005)	8.99999 × (1 ± 0.000013)	—	—	1.4×10^{-3}
(0, 0, 10, 1, 5)	1.282 × (1 ± 0.008)	13.916 × (1 ± 0.0019)	—	—	3.2×10^{-2}
(0, 0, 10, 1, 10)	2.502 × (1 ± 0.008)	16.517 × (1 ± 0.0041)	—	—	6.0×10^{-2}
(0, 0, 10, 1, 15)	8.667 × (1 ± 0.015)	2.9165 × (1 ± 0.0038)	—	—	1.9×10^{-1}
(0, 0, 10, ∞, 0)	1.06837 × (1 ± 0.0007)	6.071073 × (1 ± 0.000012)	—	—	1.8×10^{-3}
(0, 0, 10, ∞, 5)	1.1463 × (1 ± 0.0033)	4.01259 × (1 ± 0.00018)	—	—	6.3×10^{-3}
(0, 0, 10, ∞, 10)	1.2592 × (1 ± 0.0024)	2.47617 × (1 ± 0.00009)	—	—	4.0×10^{-3}
(0, 0, 10, ∞, 20)	1.4764 × (1 ± 0.0037)	1.37478 × (1 ± 0.00008)	—	—	4.7×10^{-3}
(0, 0, 10, 5, 0)	0.9784 × (1 ± 0.005)	9.00015 × (1 ± 0.00007)	0.9123 × (1 ± 0.0069)	13.76 × (1 ± 0.009)	7.3×10^{-3}
(0, 0, 10, 5, 5)	1.1312 × (1 ± 0.007)	13.8973 × (1 ± 0.0012)	1.198 × (1 ± 0.012)	10.84 × (1 ± 0.0014)	1.4×10^{-2}
(0, 0, 10, 5, 10)	2.1999 × (1 ± 0.010)	16. 4569 × (1 ± 0.0027)	2.3015 × (1 ± 0.013)	10.00 × (1 ± 0.015)	3.0×10^{-2}
(0, 0, 10, 5, 15)	3.051 × (1 ± 0.035)	2.93023 × (1 ± 0.00022)	5.719 × (1 ± 0.019)	2.835 × (1 ± 0.011)	1.1×10^{-2}
(0, 0, 1000, 1, 0)	1.0004982 × (1 ± 0.000003)	999.00000	—	—	1.4×10^{-5}
(0, 0, 1000, 1, 5)	1.00787 × (1 ± 0.0010)	1887.55 × (1 ± 0.00006)	—	—	3.8×10^{-3}
(0, 0, 1000, 1, 10)	1.0099 × (1 ± 0.0013)	6131.2 × (1 ± 0.0027)	—	—	5.0×10^{-3}
(0, 0, 1000, 1, 15)	1.0099 × (1 ± 0.0013)	21491.0 × (1 ± 0.0010)	—	—	5.1×10^{-3}
(0, ∞, 10, 1, 0)	1.02477 × (1 ± 0.00024)	18.99998 × (1 ± 0.000014)	—	—	7.8×10^{-4}

(0, ∞, 10, 1, 2.5)	0.9587 × (1 ± 0.0026)	36.617 × (1 ± 0.0025)	0.675 × (1 ± 0.0026)	19.32 × (1 ± 0.0025)	5.3×10^{-3}
(0, ∞, 10, 1, 5)	0.9113 × (1 ± 0.0030)	122.438 × (1 ± 0.0007)	0.9113 × (1 ± 0.005)	19.45 × (1 ± 0.007)	6.0×10^{-3}
(0, ∞, 10, 1, 7.5)	0.8959 × (1 ± 0.0031)	428.8557 × (1 ± 0.000017)	0.9156 × (1 ± 0.0029)	19.274 × (1 ± 0.0041)	8.1×10^{-3}
(0, ∞, 10, ∞, 0)	1.03493 × (1 ± 0.00034)	13.14212 × (1 ± 0.000013)	—	—	1.1×10^{-3}
(0, ∞, 10, ∞, 2.5)	0.9451 × (1 ± 0.0015)	36.95041 × (1 ± 0.000016)	—	—	4.3×10^{-3}
(0, ∞, 10, ∞, 5)	0.9021 × (1 ± 0.0014)	122.38693 × (1 ± 0.000006)	—	—	5.6×10^{-6}
(0, ∞, 10, ∞, 7.5)	0.8871 × (1 ± 0.0017)	426.112 × (1 ± 0.000024)	—	—	6.7×10^{-3}
(0, ∞, 10, ∞, —2.5)	1.14760 × (1 ± 0.000026)	6.297733	—	—	8.9×10^{-5}
(0, ∞, 10, ∞, —5)	1.250425 × (1 ± 0.000001)	3.962154	—	—	3.9×10^{-6}
(0, ∞, 10, ∞, —7.5)	1.342005	2.920020	—	—	1.6×10^{-7}
(0, ∞, 10, 5, 0)	0.9865 × (1 ± 0.0026)	18.9996 × (1 ± 0.00015)	0.8576 × (1 ± 0.009)	26.82 × (1 ± 0.010)	5.7×10^{-3}
(0, ∞, 10, 5, 2.5)	1.0022 × (1 ± 0.0032)	36.77101 × (1 ± 0.000005)	—	—	$16. \times 10^{-2}$
(0, ∞, 10, 5, 5)	0.8069 × (1 ± 0.010)	121.6457 × (1 ± 0.00002)	4.653 × (1 ± 0.0022)	25.826 × (1 ± 0.0031)	2.2×10^{-2}
(0, ∞, 10, 5, 7.5)	0.7944 × (1 ± 0.010)	428.856 × (1 ± 0.00007)	4.6405 × (1 ± 0.0021)	25.662 × (1 ± .0031)	2.2×10^{-2}
(0, ∞, 10, 5, —2.5)	0.8443 × (1 ± 0.010)	36.77103 × (1 ± 0.000006)	4.124 × (1 ± 0.0025)	26.3964 × (1 ± 0.0037)	2.2×10^{-2}
(0, ∞, 10, 5, —5)	0.9219 × (1 ± 0.0014)	121.64566 × (1 ± 0.000003)	0.1702 × (1 ± 0.009)	26.100 × (1 ± 0.0014)	3.7×10^{-3}
(0, ∞, 10, 5, —7.5)	0.9061 × (1 ± 0.0018)	428.8556 × (1 ± 0.000015)	0.1807 × (1 ± 0.011)	25.87 × (1 ± 0.017)	4.7×10^{-3}

roughly $[0.25(2 + \pi_m + \pi_m^{-1})]^{1/2}(2M)$, reflecting diffusion of charge through the entire system.

Unweighted fitting of the same data expressed as system admittance yields similar values of the circuit parameters but not usually agreement within the standard errors estimated for the parameters in the impedance fit. The disagreement between the impedance and admittance fits is not serious but does confirm that the equivalent circuit provides only an approximation to the exact system response (even in the flat-band $V_{as}^* = 0$ case). Care must be taken in the fitting process to include a sufficiently wide range of frequencies or spurious parameter estimates may be encountered. While it is probable that further useful refinements of the fitting process, perhaps using an alternative weighting or a modified equivalent circuit, can be achieved, the procedure adopted in this work appears to be adequate for the preliminary analysis of experimental data for appropriate systems.

(VII) SUMMARY AND CONCLUSIONS

We have reported small-signal impedance and admittance results for unsupported systems with one or two blocking electrodes subject to an external steady bias, obtained by computer solution of the appropriate differential equations. In addition to the qualitative features previously discussed for flat-band systems [34,35], the presence of an external bias induces behavior which may be attributed to the redistribution of charge and, in the case of one non-blocking electrode, to charge injection into the system. An equivalent circuit was found which provided adequate least-square fits to the system impedance and yields parameter estimates consistent with a qualitative understanding of the physical processes involved in system response.

The results presented here are most applicable to situations in which the possible presence of compact layers owing to finite ion size, specific adsorption, or system preparation (air gaps, etc.) can be neglected. In future work this restriction will be removed, and we shall examine the role of the compact layer in small-signal response for systems subject to external bias, with and without intrinsic space charge (Frenkel) layers.

ACKNOWLEDGMENT

The research for this work was supported by U.S. National Science Foundation, Grant No. 76-84187.

REFERENCES

1 G. Jaffé, Ann. Phys., 16 (1933) 217.
2 J.R. Macdonal, J. Chem. Phys., 29 (1958) 1346.
3 J.R. Macdonald, J. Chem. Phys., 30 (1959) 806.
4 J.R. Macdonald, J. Chem. Phys., 22 (1954) 1317.
5 D.R. Franceschetti and J.R. Macdonald, J. Appl. Phys., 50 (1979) 291.
6 J.R. Macdonald, J. Chem. Phys., 58 (1973) 4982.
7 J.R. Macdonald and D.R. Franceschetti, J. Chem. Phys., 68 (1978) 1614.
8 D. Kahn and J.N. Maycock, J. Chem. Phys., 46 (1967) 4434.
9 S.W. Feldberg, Electroanal. Chem., 3 (1969) 199.

10 J.R. Sandifer and R.P. Buck, J. Electroanal. Chem., 49 (1974) 161.
11 T.R. Brumleve and R.P. Buck, J. Electroanal. Chem., 90 (1978) 1.
12 J.R. Macdonald, Solid State Electron., 5 (1962) 11.
13 H.K. Gummel, IEEE Trans. Electron Devices, ED-11 (1964) 455.
14 A. De Mari, Solid State Electron, 11 (1968) 1021.
15 M. Kurata, IEEE Trans. Electron Devices, ED-19 (1972) 1207.
16 C.M. Lee, R.J. Lomax and G.I. Haddad, IEEE Trans. Microwave Theory and Techniques, MTT-22 (1974) 160.
17 D.Y. Wang, D. Eng. Sci. Thesis, Krumb School of Mines, Columbia University, New York, 1978.
18 D.Y. Wang and A.S. Nowick, J. Electrochem. Soc., to be published.
19 J. Bert, Ph. D. Thesis, Université Claude Bernard, Lyon, France, 1978.
20 R.D. Armstrong, R.A. Burnham and P.M. Willis, J. Electroanal., Chem., 67 (1976) 111.
21 N. Rosenberg, private communication.
22 A. Erdélyi, W. Magnus, F. Oberhettinger and F.G. Tricomi, Higher Transcendental Functions, Vol. II, McGraw-Hill, New York, 1953, p. 294 ff.
23 J.R. Macdonald, J. Appl. Phys., 46 (1975) 4602.
24 N.L. Schryer, Bell Laboratories Computing Science Technical Report No. 53, 1977.
25 N.L. Schryer, Bell Laboratories Computing Science Technical Report No. 52, 1977.
26 P.A. Fox, A.D. Hall and N.L. Schryer, Bell Laboratories Computing Science Technical Report No. 47, 1976.
27 D.R. Franceschetti and J.R. Macdonald, J. Electroanal. Chem., 82 (1977) 271.
28 J. Frenkel, Kinetic Theory of Liquids, Oxford Univeristy Press, New York, 1946, p. 36.
29 J.R. Macdonald, J. Appl. Phys., 43 (1972) 1457.
30 J.R. Macdonald, J. Electroanal. Chem., 32 (1971) 317.
31 D.R. Franceschetti and J.R. Macdonald, J. Electroanal. Chem., in press.
32 J.R. Macdonald and J.A. Garber, J. Electrochem. Soc., 124 (1977) 1022.
33 J.C. Slater, Microwave Transmission, McGraw-Hill, New York, 1942, p. 17 ff.
34 J.R. Macdonald, J. Electroanal. Chem., 53 (1974) 1.
35 J.R. Macdonald, J. Chem. Phys., 61 (1974) 3977.